Journal of Power Sources 196 (2011) 2135–2142

Contents lists available at ScienceDirect

Journal of Power Sources

journal homepage: www.elsevier.com/locate/jpowsour

Stabilizing lithium plating-stripping reaction between a lithium phosphorus oxynitride glass electrolyte and copper thin film by platinum insertion

Kengo Okita [a], Ken-ichi Ikeda [a], Hikaru Sano [b,c], Yasutoshi Iriyama [a,b,*], Hikari Sakaebe [b,c]

[a] Department of Materials Science and Chemical Engineering, Faculty of Engineering, Shizuoka University, 3-5-1 Johoku, Naka-ku, Hamamatsu, Shizuoka 432-8561, Japan
[b] JST, CREST, 5 Sanbancho, Chiyoda-ku, Tokyo 102-0075, Japan
[c] Research Institute for Ubiquitous Energy Devices, National Institute of Advanced Industrial Science and Technology (AIST), Midorigaoka 1-8-31, Ikeda, Osaka 563-8577, Japan

ARTICLE INFO

Article history:
Received 23 September 2010
Received in revised form 1 October 2010
Accepted 1 October 2010
Available online 11 October 2010

Keywords:
All-solid-state lithium batteries
Lithium metal anode
Thin film
Interface

ABSTRACT

Lithium (Li) plating-stripping reaction properties at the lithium phosphorus oxynitride glass electrolyte (LiPON)/copper thin film (Cu) interface is improved by the insertion of nano-thickness platinum (Pt) layer at the interface. The LiPON films are formed on mirror-polished lithium-ion conductive solid electrolyte sheets, and current collector thin films of Li, Cu–Pt multi layer, and Cu are formed on the LiPON films. The plating-stripping reactions at the LiPON/current collector films interface are carried out by galvanostatic and potential sweep measurements. Galvanostatic measurements reveal that Pt layer insertion reduces the overvoltage of the reaction and improves its coulomb efficiency. Also, cyclic voltammetry measurement suggests formation of Li–Pt alloys at higher voltages than 0 V (vs. Li/Li^+) during the lithium plating process. Scanning electron microscopy observation clarifies that platinum insertion moderate non-uniform lithium plating reaction. Most probably, Li–Pt alloys increase the reaction sites, resulting in both the stabilization of current collector and the reduction of the overvoltage of the lithium plating-stripping reaction upon cycling. The results shown here will be useful in improving the anode reaction of the "Li-free" all-solid-state lithium batteries.

1. Introduction

The development of rechargeable lithium batteries with high energy densities is under strong demand, especially for their application as a power source of electric and hybrid vehicles. Lithium metal anode possesses an energy density that is about 10 times larger (3860 mAh g^{-1}) than the conventional graphite anode. The use of lithium metal anode in rechargeable lithium batteries must be effective for the development of batteries with high energy densities [1].

Although rechargeable lithium batteries with lithium metal anode were manufactured before 1990, most did not obtain sufficient cycle life (ca. 300 cycles) [2]. In addition, repeated lithium plating-stripping reactions during the charge–discharge process induced morphology changes on the electrode surface, typically a dendritic growth of lithium metal. The resultant fine particles removed from the substrate or the dendrite growth to the cathode could lead to an internal short circuit of the battery, resulting in an accident, such as huge heat generation and fire. This short-circuit problem has been identified even in rechargeable lithium batteries using polymer electrolytes [3]. However, lithium metal has been used successfully as an anode material in thin-film all-solid-state batteries (TFBs) using inorganic solid electrolytes [4–7], and some of these batteries have achieved charge–discharge reactions over 40,000 times without a large capacity loss [8]. Moreover, application of non-flammable inorganic solid electrolytes in place of flammable organic electrolytes will overcome the safety problems of the battery. Therefore, inorganic solid electrolytes will be key materials in the realization of high energy density rechargeable lithium batteries with lithium metal anode.

Among the various kinds of inorganic solid electrolytes, lithium phosphorus oxynitride glass electrolyte (LiPON: $\sigma_{RT} = 2 \times 10^{-6}$ S cm^{-1}) has unique stability with lithium metal [9] and is one of the most famous solid electrolytes applied in TFBs. In such TFBs, lithium metal anode is commonly used, and the batteries have excellent charge–discharge properties [4–7], indicating that the lithium plating-stripping reaction at the LiPON/lithium metal interface can take place with high efficiency. However, for practical application, use of electroplated lithium metal is attractive for simplifying the battery manufacturing process, reducing the fabrication cost, and facilitating battery treatments. These Li-free TFBs, using *in situ* electroplated lithium metal anode, were first proposed by Neuecker et al. [10]. This group assembled a $Cu/LiPON/LiCoO_2$ multi-layer and formed an electroplated lithium

* Corresponding author at: Department of Materials Science and Chemical Engineering, Faculty of Engineering, Shizuoka University, 3-5-1 Johoku, Naka-ku, Hamamatsu, Shizuoka 432-8561, Japan. Tel.: +81 53 478 1168; fax: +81 53 478 1168.
E-mail address: tyiriya@ipc.shizuoka.ac.jp (Y. Iriyama).

0378-7753/$ – see front matter © 2010 Elsevier B.V. All rights reserved.
doi:10.1016/j.jpowsour.2010.10.014

metal anode at the Cu/LiPON interface. The resultant TFBs showed large irreversible capacity losses in the initial charge–discharge process, and their cycle performances were also inferior to those with lithium metal anodes (Li/LiPON/$LiCoO_2$). Surface coating by parylene or LiPON on the Cu film [10] or lithium plating under LiPON film [11] improved these unfavorable properties, but the resultant systems are still inferior to the TFBs with lithium metal anode. To overcome this lower lithium plating-stripping property, the *in situ* electroplating reaction of lithium on a heterogeneous current collector should be improved.

It is well known that the lithium plating-stripping reaction has been improved by the addition of appropriate additives and pressures, in the case of the liquid electrolyte system [12]. In the case of the polymer electrolyte system, insertion of a lithium alloy between the lithium anode and the polymer electrolyte was effective in stabilizing the lithium plating-stripping reaction and reducing the overvoltage [13]. According to these results, the regulation of interfacial reactions might also improve the lithium plating-stripping reaction for the glass electrolyte system. The lithium plating-stripping reactions in Li-free TFBs have been carried out on copper [10] and stainless steel substrates [11,14], but the effects of the current collector species on its reaction properties have not been discussed. Thus, in the present work, we prepared a LiPON thin film on a mirror-polished glass ceramic solid electrolyte sheet with a NASICON-based structure (OHARA sheet, manufactured by OHARA Inc., Kanagawa, Japan [15]), and different kinds of current collector films were mounted on the LiPON films. Here, we focused on platinum that forms lithium–platinum alloys, and the effects of platinum insertion between the LiPON and the copper thin film on the reaction properties were investigated. This binary system forms various kinds of alloy phases (e.g., Li_9Pt, Li_5Pt, $Li_{15}Pt_4$, and Li_2Pt [16]), and the storage number of lithium atoms per atom can exceed that of Si (e.g., $Li_{21}Si_5$ and $Li_{13}Si_4$ [17]) and Sn (e.g., $Li_{17}Sn_4$ and Li_7Sn_2 [18]). This property will be helpful in investigating the effect of the alloying metal layer insertion between the LiPON and the current collector film on the electrochemical lithium plating-stripping reaction properties. Finally, we will show that insertion of an appropriate amount of platinum can improve the *in situ* lithium plating-stripping reaction.

2. Experimental

Thin films of LiPON (2–3 μm in thickness) were deposited on one side of the OHARA sheet (150 μm in thickness, $\sigma_{298K} = 1 \times 10^{-4}$ S cm^{-1} [15]) by RF magnetron sputtering. The LiPON films were prepared following the methods reported by Bates et al. [9,19]. Thin films of copper or platinum were prepared by pulsed laser deposition (PLD) on the LiPON films. The fourth harmonic of a YAG laser was focused on the metal sheet targets with a 10 Hz repetition rate so that the energy density was 2.5 J cm^{-2} on the target surface. The deposition chamber was filled with argon, and the pressure was maintained at 2.7 Pa during the deposition. Thin films of copper were deposited for 40 min in every case. Platinum thin films were also deposited by PLD between copper thin films and LiPON films under the same preparation conditions for 0.5, 2, 5, or 10 min. The thickness of these films was estimated from the depth profile of Auger electron microscopy (AES). Lithium thin films were deposited on the LiPON films by vacuum evaporation equipped in an argon-filled grove box. As a result, LiPON/OHARA sheet multi-layered solid electrolyte sheets equipped with different current collector films of copper, platinum–copper multi-layer, and lithium were fabricated, and these sheet cells will be henceforth referred to as Cu-cell, Cu–Pt(x)-cell (where x denotes deposition minutes of platinum film), and Li-cell, respectively.

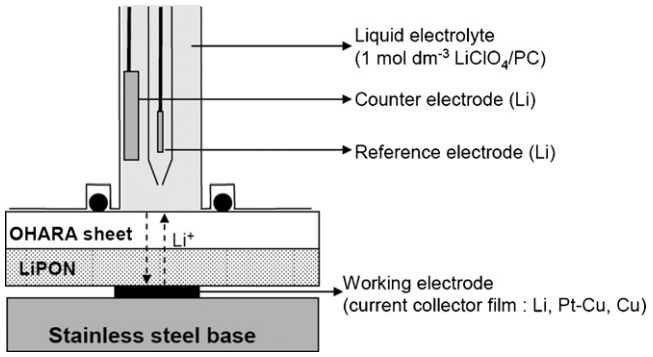

Fig. 1. Schematic image of the three-electrode cell for the lithium plating-stripping reaction in the multi-layered solid-state half cells (OHARA-sheet/LiPON film/current collector films of copper, platinum–copper multi-layers, or lithium).

Electrochemical lithium plating-stripping reactions on the above sheet cells were conducted using a three-electrode cell. Fig. 1 shows the schematic image of the electrochemical measurement cell, where the sheet cells are set at the bottom of the electrochemical cell so that bare side of the OHARA sheet is immersed in 1 mol dm^{-3} $LiClO_4$ dissolved in propylene carbonate (PC). The working electrode was a current collector film that was mounted on a stainless steel base, and both counter and reference electrodes were lithium metal. Hereafter, all the electrode potentials will be referred to Li/Li$^+$. Lithium ions pass through the multi-layered solid electrolyte sheet, and its plating-stripping reaction occurs at the LiPON/current collector film interface. The lithium plating reaction was carried out at a constant current of 50 μA cm^{-2} for 30 min in all cases (theoretical amount of electroplated lithium film: 0.127 μm cm^{-2}). The stripping reaction was conducted at the reverse current density until the electrode potential attained 3.0 V for the Cu- and Cu–Pt-cells, while the current flow time was limited to 30 min for the Li-cells. These reactions were cycled 50 times at room temperature in an argon-filled grove box. AC impedance spectroscopy was measured at open circuit voltages during the above reactions. The impedance was measured by applying a sine wave of 10 mV amplitude over the frequency range of 200 kHz to 100 mHz. Cyclic voltammetry measurements were carried out in both the Cu-cells and Cu–Pt(5)-cells between 3.0 V and −0.1 V at a potential sweep rate of 0.1 mV s^{-1}.

The current collector films before and after the reactions were observed by scanning electron microscopy (SEM) without exposing the samples to air. AES was applied to investigate the distribution of copper and platinum in the Cu–Pt(10)-cell at the initial state and after the 50th lithium plating reaction. The sheet cells were sliced into wedge shapes, and the AES measurement was conducted in the vicinity of the LiPON/current collector film interface on the sliced surface. The details of the AES measurements will be described in the section below.

3. Results and discussion

3.1. Thickness of the current collector films in the sheet cells

Fig. 2 shows the atomic concentration profile of the copper and platinum thin films in the Cu–Pt(10)-cell measured by the AES depth profile. The current collector film was etched from the surface by argon ions at a rate of 6 nm min^{-1} in SiO_2, and layers of copper, platinum, and LiPON films were observed sequentially. From this result, the thickness of the copper and platinum films in the Cu–Pt(10)-cell were estimated as 8 and 40 nm, respectively, by considering the sputtering ratio of each material against SiO_2. The thickness of the lithium film in the Li-cell was measured as 4–5 μm from the cross-sectional SEM image, as described below.

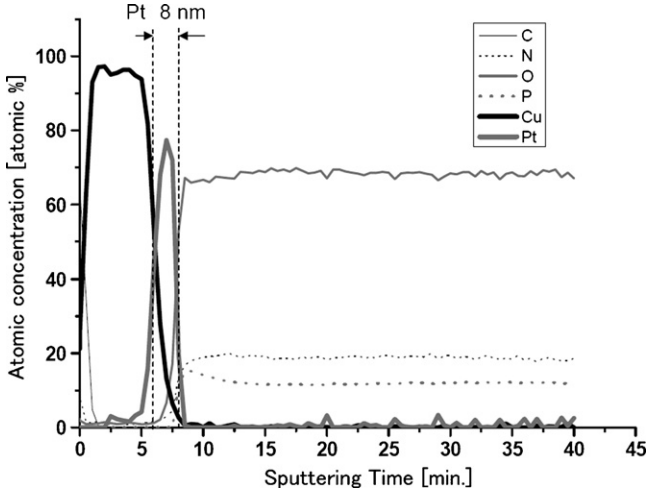

Fig. 2. Auger depth profile of a copper–platinum multi-layer/LiPON/OHARA sheet half cell. Both copper and platinum films were prepared by pulsed laser deposition. The platinum thin film was deposited on LiPON film for 5 min, and the copper was deposited for 40 min on the resultant platinum film.

3.2. Lithium plating-stripping curves of the sheet cells

Fig. 3 shows the lithium plating-stripping curves of the Cu-, Cu–Pt(5)-, and Li-cells at the 1st, 10th, 20th, 30th, 40th, and 50th cycles. The *x*-axis in Fig. 3 indicates the total current flow time in each cycle, and the plating reactions were switched to stripping reactions at 1800 s. Magnified plating curves are also displayed in the inset of each figure. Fig. 3(a) shows the plating-stripping curves of the Cu-cell, which could not repeat a stable reaction. In the stripping curves of the Cu-cell, the potential plateau region around 0 V decreased with each cycle, while the capacity above 0 V increased. At the plating reaction of the Cu-cell, the overvoltage after the 1st plating reaction (ΔV_1) was 40 mV, while the value after the 50th plating reaction (ΔV_{50}) was 49 mV. The coulomb efficiency of a stripping reaction up to 1.0 V ($Q_{st\ 1.0V}$) against the plating reaction (Q_{pl}) was 84.7% at the 1st cycle and decreased to 53.4% at the 50th cycle. These results indicate that the lithium plating-stripping reaction in the Cu-cell becomes highly resistive and unstable as the number of cycles increases. On the other hand, the plating-stripping reaction curves were stabilized in the Cu–Pt(5)-cell, as shown in Fig. 3(b), where a nano-thickness plat-

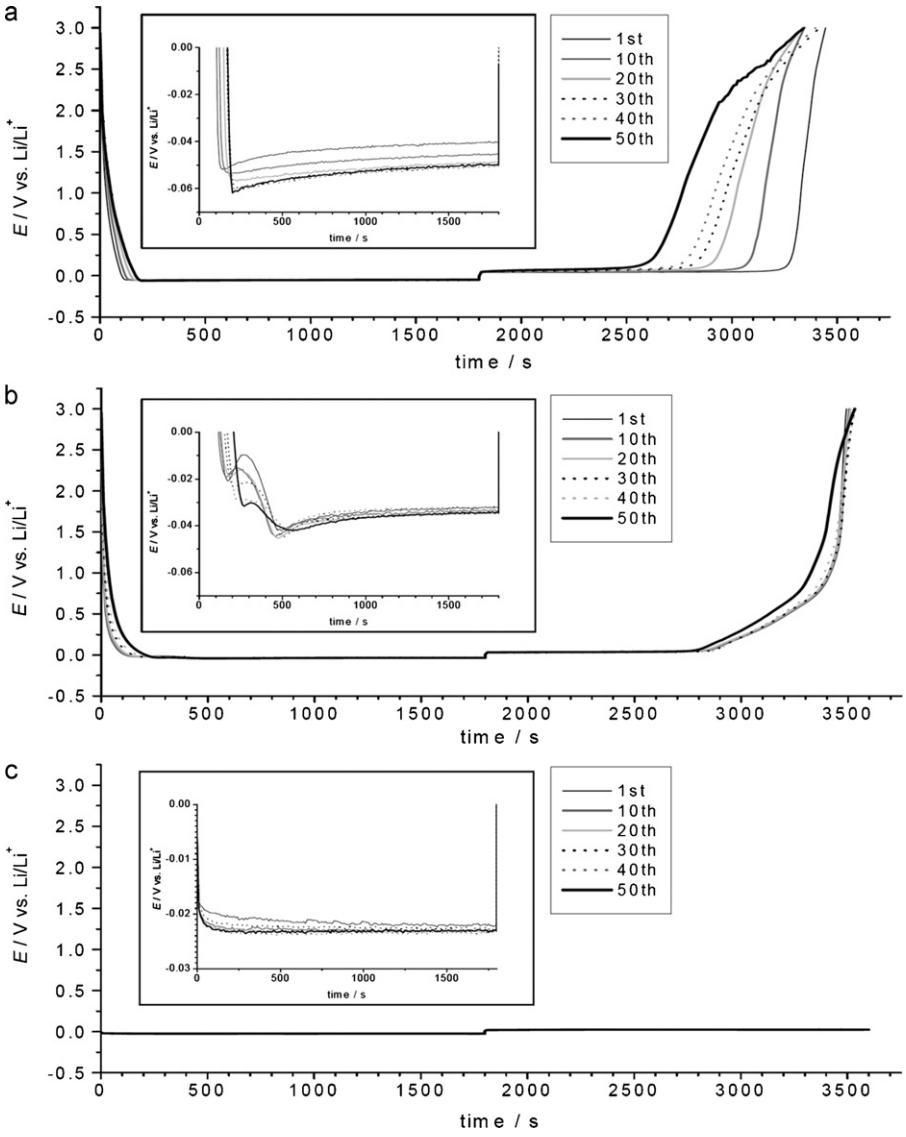

Fig. 3. Lithium plating-stripping curves in the current collector films/LiPON/OHARA sheet half cells for 50 cycles, where the current collector film was (a) copper, (b) copper–platinum (5 min deposition by pulsed laser deposition) multi-layer, and (c) lithium; 1st (black thin solid line), 10th (gray thin solid line), 20th (gray narrow line), 30th (black dotted line), 40th (gray dotted line), and 50th (black bold line) cycle. The inset in each figure shows the magnified plating curves in each cell. $I = 50\ \mu A\ cm^{-2}$.

inum layer was inserted between the LiPON and the copper film. The ΔV_1 decreased to 32 mV, and the ΔV_{50} slightly increased to 34 mV. The coulomb efficiency ($Q_{st\ 1.0V}/Q_{pl}$) at the 1st cycle was 89.7%, which slightly decreased to 84.6% at the 50th cycle. As shown in the inset of Fig. 3(b), potential spikes were observed at the initial plating reaction, similar to the Cu-cell.

Fig. 3(c) shows the plating-stripping curves of the Li-cell. Potential plateaus were observed near 0 V in both plating and stripping reaction. Stable plating-stripping reactions were repeated for 50 cycles, and those curves were therefore overlapped in this scale. As shown in the inset of Fig. 3(c), the ΔV_1 was the smallest at 22 mV, in the three cells, and the ΔV_{50} increased slightly to 23 mV. The coulomb efficiency of the stripping reaction against the plating reaction was 100% as a calculated value in these cycles. At the initial plating reaction, a potential spike was observed in both the Cu- and Cu–Pt(5)-cells but not in the Li-cell. Thus, this potential spike might be ascribed to the nucleation reaction of the lithium plating reaction at the LiPON/current collector film interface.

AC impedance spectra were measured during these plating-stripping reactions. The Cole–Cole plot measured at 3.0 V in the Cu-cell (Fig. 4(a)) was composed of one semicircular arc followed by a nearly vertical line to the real axis, which was typical of a blocking electrode system. In this equivalent circuit model, the various parallel units of the resistance and capacitance (or constant phase element) must be connected in series: generated from lithium ion transfer in the liquid electrolyte, at the liquid electrolyte/OHARA sheet interface, in the OHARA sheet, at the OHARA sheet/LiPON interface, and in the LiPON film. However, these semicircular arcs were not well separated, and thus their mixing components appeared as one semicircular arc. After 1800 s of the lithium plating reaction, a second semicircular arc appeared in a lower frequency region, resulting in the typical shape of a non-blocking electrode system. This second semicircular arc is assigned to the charge transfer reaction at the LiPON/electroplated lithium interface. However, the diameters of these two semicircular arcs increased after the 50th cycle, indicating that the internal resistance of the Cu-cell increased as the number of cycles increased. Very similar spectra were observed in the Cu–Pt(5)-cell, as shown in Fig. 4(b). The diameter of the semicircular arc in the high frequency region was nearly identical with that of the Cu-cell, while that of the second semicircular arc was about a half of that of the Cu-cell. These results indicate that charge transfer resistance was reduced by the presence of the platinum layer. The cycle-to-cycle variation of these semicircular arcs was suppressed compared with the Cu-cell.

The Li-cell spectrum was composed of two semicircular arcs in the pristine state because the lithium metal film (non-blocking electrode) was initially formed on the LiPON film. As shown in Fig. 4(c), the diameter of the semicircular arc in the high frequency region was consistent with other cells, indicating that the resistance in this semicircular arc was identical with that in the other two cells. However, the diameter of the second semicircular arc had the smallest value in the three cells, and the variation in these arcs was negligibly small after the cycles. This result means that lithium plating-stripping reactions can occur stably and with low resistance in the Li-cell.

The order of stability of lithium plating-stripping reaction with the cycles expected from Fig. 3 is Li-cell > Cu–Pt(5)-cell > Cu-cell; this order is in reasonable agreement with the results of the AC impedance measurements shown in Fig. 4.

3.3. Surface morphology and the element distribution in the electroplated lithium film

A morphology change of the current collector film upon lithium plating-stripping was observed by SEM, in which the surface of each half cell was observed from the bottom side in Fig. 1. As shown

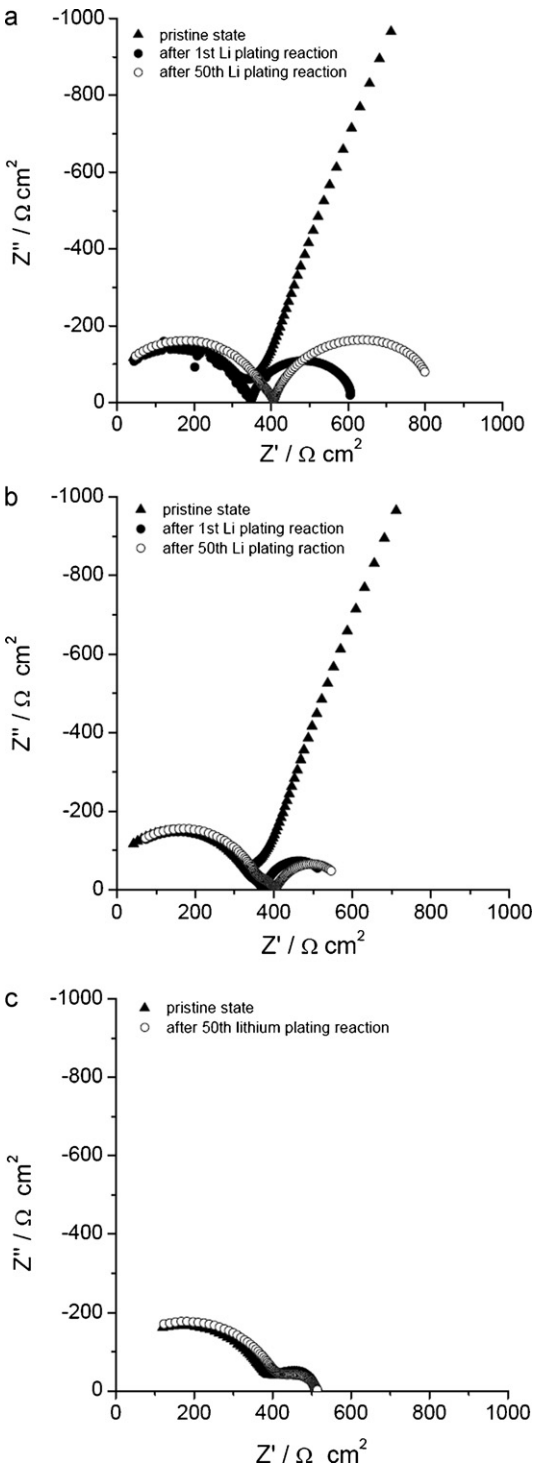

Fig. 4. Cole–Cole plots measured at the pristine state (triangles), after the 1st lithium plating reaction (closed circles), and after the 50th lithium plating reaction (open circles) of the current collector films/LiPON/OHARA sheet half cells, in which the current collector film was (a) copper, (b) copper–platinum (5 min deposition by pulsed laser deposition) multi-layer, and (c) lithium.

below, the electroplated lithium grew towards the current collector film from LiPON film, which was contrary to the situation in the liquid electrolyte system. Fig. 5 shows the SEM images of the lithium metal film in the Li-cell before and after 50 cycles of the plating-stripping reaction. A smooth surface morphology with a uniform thickness of 4–5 μm was observed in the pristine lithium film (Fig. 5(a) and (b)). After the 50th lithium plating reaction, the

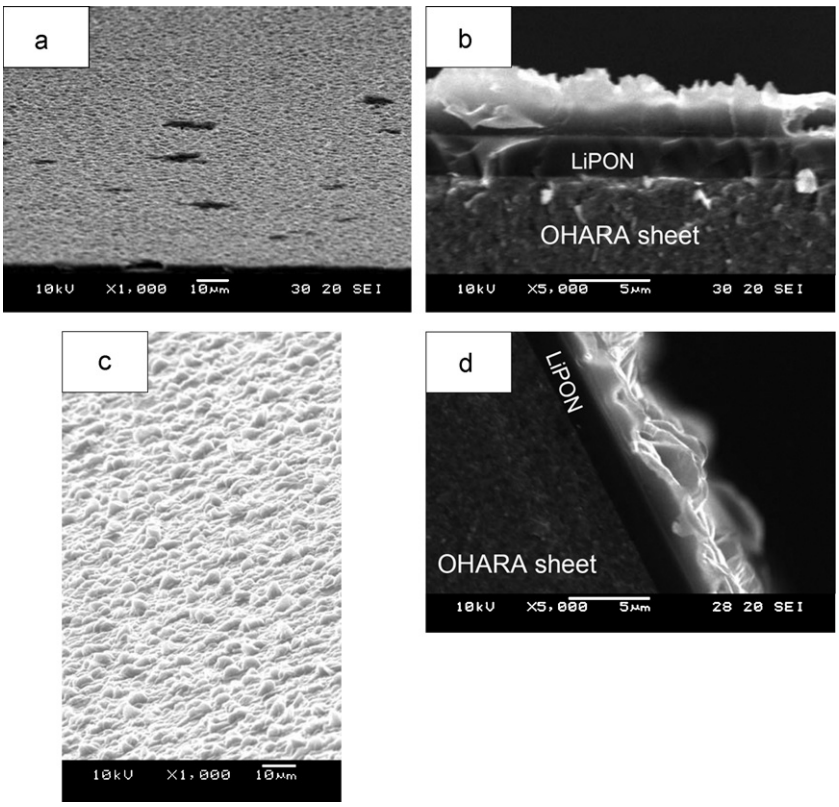

Fig. 5. SEM images of the lithium metal film in the Li/LiPON/OHARA half cell before (a and b) and after (c and d) 50 cycles of the plating-stripping reaction. (a) and (c) are the surface images, and (b) and (d) cross-sectional images.

surface morphology became rough (Fig. 5(c)), and the film thickness distribution was also observed in a cross-sectional SEM image (Fig. 5(d)). Grain growth in the lithium metal film occurred during the cycles as shown in Fig. 5(d).

Fig. 6 shows the SEM images of the Cu- and Cu–Pt(5)-cells. The pristine surface of the current collector film was flat in both cells as shown in Fig. 6(a). After the 50th cycle in the Cu-cell, an inhomogeneous hill-like texture of a few tens of microns in height appeared (Fig. 6(b) and (c)), while the surface in the Cu–Pt(5)-cell was composed of fine grains and a minor amount of needle-like precipitation over the whole area (Fig. 6(d)–(f)). Also, in both cases, electroplated lithium grew towards the current collector film from LiPON film, which is contrary to the situation in the liquid electrolyte.

AES measurements were performed to investigate the distributions of platinum and copper in the Cu–Pt(5)-cell at the initial state (Fig. 7(a)–(c)) and after the 50th lithium plating reaction (Fig. 7(d)–(f)). Fig. 7(a) and (d) shows the schematic images of the wedge-cutting samples for the AES measurements, and Fig. 7(b) and (e) display the SEM images of the cutting surface. AES signals were corrected in each square numbered in Fig. 7(b) and (e), which are summarized in Fig. 7(c) and (f), respectively. The initial sample had a platinum rich region near the LiPON/current collector film interface as expected from the result in Fig. 2. However, the sample after the 50th lithium-plated state did not show an AES platinum signal near the interface or in the middle of the electroplated lithium film, probably due to very small concentration of platinum. The platinum most likely diffused into the electroplated lithium film during the lithium plating-stripping cycles. The AES signal from copper decreased after the 50th lithium plating reaction. An increased surface roughness on the cutting surface will partly contribute to the decrease of signal, but the apparent density of the copper film also may change from the initial state.

4. Discussion

The lithium plating-stripping reaction on lithium metal in the Li-cell showed stable and only mildly resistive performance in these cells. This result is consistent with the excellent charge–discharge reactions in various TFBs with lithium metal anode [4–7]. At the initial lithium plating process, potential spikes were not observed in the Li-cell, which means that the nucleation reaction does not occur in this growth process. Thin lithium films form in a polycrystalline state, and there must be many steps and kink sites at the LiPON/Li interface. Following the classical terrace-step-kink model for the electroplating-stripping reaction mechanism, lithium will grow in many steps or kink sites, and the nucleation-growth reaction will not be preferential at small overvoltages [20]. In the SEM image, grain growth in the lithium film was observed after the cycles, suggesting that defects present inside the initial lithium metal film are partly removed during the cycles.

An inhomogeneous lithium plating reaction was observed in the Cu-cell, which was moderated by the insertion of a thin platinum layer between the copper and LiPON films. Fig. 8 shows the cyclic voltammograms (CVs) of both the Cu- and Cu–Pt(5)-cells measured between 3.0 and −0.1 V at a potential sweep rate of 0.1 mV s^{-1}. Two peaks were observed in the Cu–Pt(5)-cell, but not the Cu-cell, at voltages above 0 V. This result suggests that platinum–lithium alloy phases are formed during the lithium plating process. In fact, several kinds of platinum–lithium alloy phases have been reported [16] that support this hypothesis. Although a copper–lithium solid solution phase has been reported in a copper–lithium binary system [21], this solid solution phase will not be preferentially formed in this case because there are no suggestive peaks in the CV. According to the Nernst equation, lithium plating on lithium metal can be

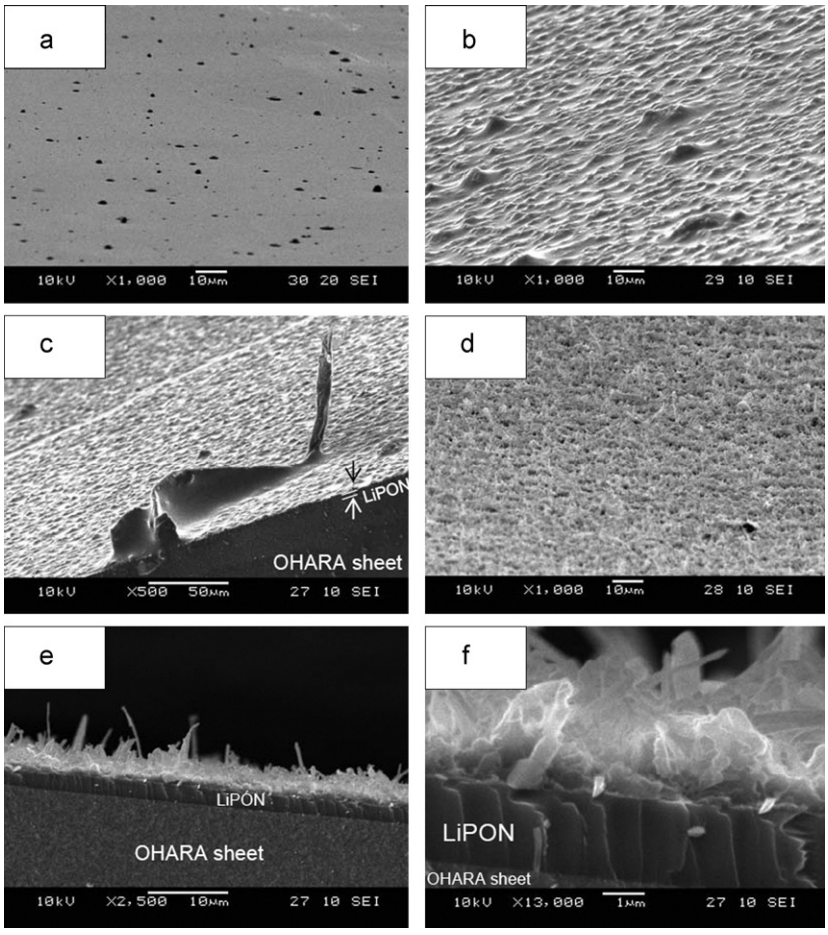

Fig. 6. SEM images of the current collector film/LiPON/OHARA sheet half cell (a) at the pristine state and (b–f) after the 50th lithium plating reactions, where the current collector film was (a–c) copper and (d–f) copper–platinum (5 min deposition by pulsed laser deposition) multi-layer. (a), (b), and (d) are surface images, while (c), (e), and (f) are cross-sectional images.

written as follows:

$$E_1 = E_0 + \frac{RT}{F} \ln \frac{a_{Li^+}}{a_{Li}}$$

where E_0 is the equilibrium electrode reaction of Li/Li^+, R is the gas constant, T is the absolute temperature, a_{Li} is the lithium activity of lithium metal, and a_{Li^+} is the lithium ion activity in the solid electrolyte. Here, a_{Li} is unity for lithium metal. However, this activity can be reduced in platinum–lithium alloys, and the above equation is written as follows:

$$E_2 = E_0 + \frac{RT}{F} \ln \frac{a_{Li^+}}{a_{Pt-Li}}$$

where a_{Pt-Li} is the lithium activity in a platinum–lithium alloy. Lithium activity in the alloys will be less than 1, and, in the equilibrium state, the lithium plating reaction on the platinum–lithium alloys occurs at a more positive potential than that on the lithium metal:

$$\Delta E = E_2 - E_1 = -\frac{RT}{F} \ln a_{Pt-Li}$$

When platinum–lithium alloys are formed, the subsequent lithium plating reaction occurs to cover the alloy phases at relatively low current density (nearly at equilibrium state). Once a thin lithium layer is formed between the LiPON and the alloy electrode films, a subsequent lithium plating-stripping reaction must occur with high stability and low resistance as with the Li-cell. This occurrence may explain the reduction of the overvoltage and the moderation of the inhomogeneous lithium plating reaction. As clarified by the AES data, a platinum-concentrated region was not present near the interface, and, most probably, the platinum was dispersed in the electroplated lithium film during the reactions. Therefore, the role of the platinum layer is to effectively fabricate lithium plating sites at an early stage in the plating-stripping cycles. Also, the electroplated lithium was composed of fine grains and needle-like precipitation after the 50th lithium plating reaction in the Cu–Pt(5)-cell, while the Li cell was not. The dispersed platinum in the plated lithium film may have disarranged the grain growth.

As observed by SEM, the electroplated lithium grew towards the current collector film from the LiPON film in both the Cu- and Cu–Pt-cells. Terabe et al. reported that Ag atomic filaments can be prepared inside the Ag^+ conductive solid-state mixed-conductor thin film (Ag_2S) during the reduction of Ag^+, which means that the Ag plating occurs towards the electrolyte side as in the liquid electrolyte system [22]. However, if similar lithium growth occurs in the LiPON film, a short circuit of the TFBs will occur easily. This situation is very difficult to image because many TFBs with LiPON solid electrolytes and lithium metal anode can repeat excellent charge–discharge reactions without short circuits. In addition, lithium can permeate through the copper film [10,23]. Therefore, the lithium can find free space for its electrochemical growth towards the current collector film and not in the LiPON film, resulting in unique lithium plating growth contrary to that in liquid or polymer electrolyte systems.

The lithium plating amount investigated in this work was $0.127\,\mu m\,cm^{-2}$, and the plating reaction was carried out for

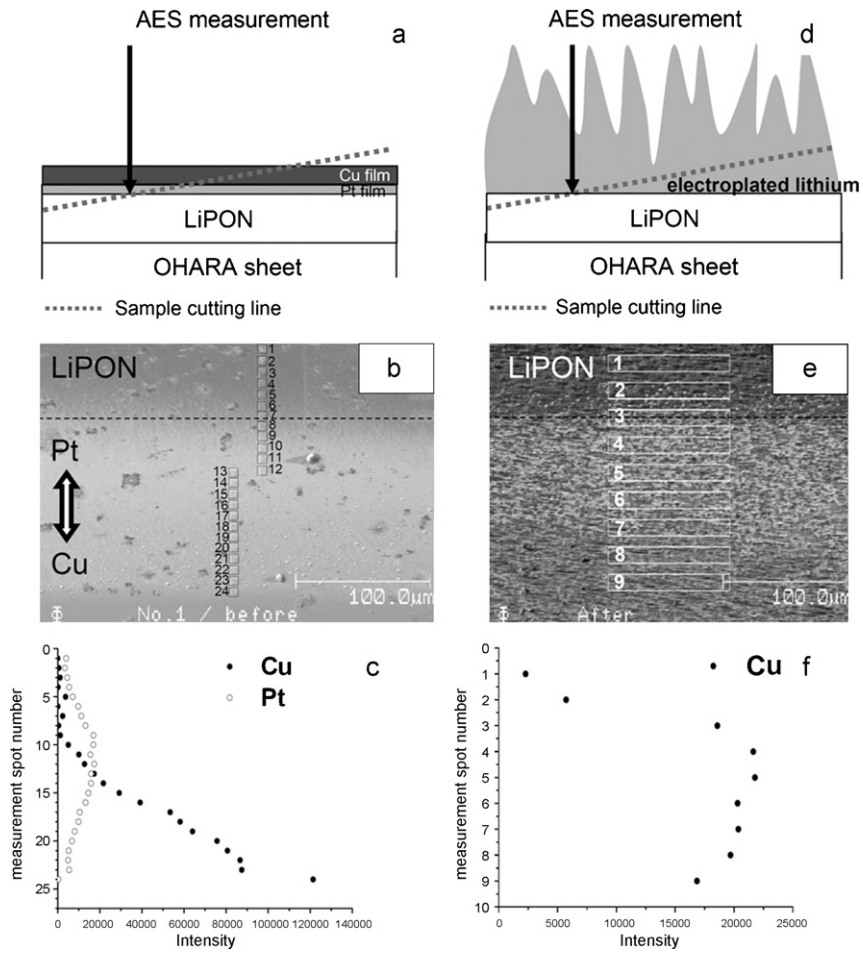

Fig. 7. Auger electron microscopy of the copper-platinum (platinum deposition time by PLD was 10 min) multi layer/LiPON/OHARA sheet half cell (a–c) at the initial state and (d–f) after the 50th lithium plating reaction. Both (a) and (d) shows the schematic image of the wedge-cutting of the above sheet cells. Both (b) and (e) shows the SEM images measured around the LiPON/platinum interface in each cell, and both (c) and (f) are the Auger intensity profiles of copper and platinum, measured from each square numbered in (b) and (e), respectively. The data in (f) do not show a platinum peak due to the detect limitation, probably caused by very low concentrations.

1800 s. These conditions correspond to electroplated lithium extracted from an approximately 0.35 μm $LiCoO_2$ thin film cathode (150 mAh g^{-1}) at a 2 C rate. This reaction rate during the charging (lithium-plating) process is comparable with those reported by Neudecker et al. [10], but the plating amount is about 1/10 of their batteries. Even in such small amounts of lithium plating, inhomogeneous plating reactions occur in the Cu-cell. Although the inhomogeneous reaction is influenced by the distribution of lithium transfer sites at the OHARA sheet/LiPON interface [21], our results clarify that the lithium plating-stripping reaction properties also depend on the species of the current collector film. Based on the SEM observations, the preferential growth of lithium occurs at the nucleated sites under this lower overvoltage. A gradual decrease in the overvoltage for each plating reaction step is explained by the increase in the number of edges sites during the growth of the nucleated part. However, AC impedance data clarified the increase in the internal cell resistance in the Cu-cell as the cycle number increases. An inhomogeneous reaction may have formed cleaved bonds between the copper and LiPON films [10] or cracking areas in copper film [22], and the resultant electrically resistive or isolated part of the copper film might be the source of increasing resistance. This finding can explain the increase of the semicircular arc in the high frequency region in the Cole–Cole plots after the reactions. Insertion of a platinum layer between the copper and LiPON films moderated the formation of the inhomogeneous reaction parts, which will be helpful in preventing the formation of electronically resistive regions in the current collector film.

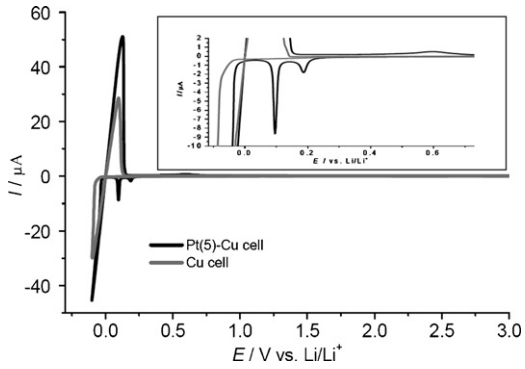

Fig. 8. Cyclic voltammograms of current collector film/LiPON/OHARA sheet half cells measured between 3.0 and −0.1 V (vs. Li/Li^+) at a potential sweep rate of 0.1 mV s^{-1}. The current collector film was copper–platinum (black: platinum deposition time by PLD was 5 min) and copper (gray) film. The inset shows the magnified image around 0 V.

Fig. 9 shows the effects of platinum deposition time on the lithium plating-stripping reaction for 30 cycles. The Cu–Pt(0.5)-cell showed nearly the same degradation as the Cu-cell, and this property was improved by increasing the platinum deposition time. Because the thickness of the platinum thin film is 8 nm even after 10 min of deposition, a shorter platinum deposition time will not be unable to coat the LiPON surface, resulting in degradation as with

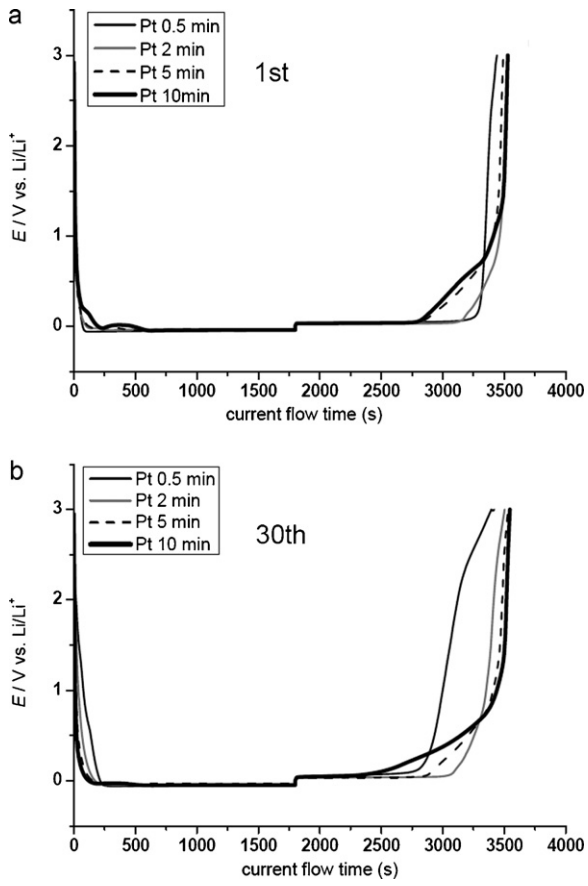

Fig. 9. Lithium plating-stripping curves of the multi-layered solid state half cell with a copper–platinum current collector thin film where platinum film was deposited for 0.5 min (black thin solid line), 2 min (gray thin solid line), 5 min (black dotted line), and 10 min (black bold line) at the (a) 1st and (b) 30th cycle. $I = 50\ \mu A\ cm^{-2}$.

the Cu-cell. When the deposition time of platinum film exceeded 5 min, the plating-stripping reaction was stabilized. However, a larger amount of platinum increased the lithium stripping potential over the course of many cycles, as shown in Fig. 9(b). In a thicker platinum film, most of the lithium may be stripped from the platinum–lithium alloys in which the lithium activity is smaller than unity, resulting in an increase in lithium stripping potential. The platinum thickness is another important factor in decreasing the voltage of the lithium stripping reaction and improving the reaction stability.

5. Conclusions

To improve lithium plating-stripping reactions at the lithium phosphorus oxynitride glass electrolyte (LiPON)/copper thin-film interface, thin platinum layers of less than 10 nm in thickness were inserted at the interface. The platinum layer will form platinum–lithium alloys by the lithium plating reaction, which increases the lithium plating sites between the LiPON and the current collector film, resulting in both the stabilization of current collector and the reduction of the overvoltage of the lithium plating-stripping reaction upon cycling. According to the AES results, platinum layer in increasing the plating sites will work effective at the early stage of the plating-stripping reaction.

The results shown here will be useful in improving the anode reaction of the "Li-free battery", where the lithium metal anode is electrochemically prepared due to the removal of lithium-ion from positive electrode materials. Although platinum is a very expensive metal, we believe that there are other elements that can stabilize the *in situ* lithium plating-stripping reaction, and its important key will be the formation of alloys with lithium metal.

Acknowledgements

The authors would like to express great appreciation to Mr. Hirofumi Yamamoto for technical support for the SEM observations. This work was financially supported by JST-CREST and also partially by NEDO (RISING).

References

[1] J.M. Tarascon, M. Armand, Nature 414 (2001) 359.
[2] K. Brabdt, Solid State Ionics 9 (1994) 173.
[3] M. Dolle, L. Sannier, B. Beaudoin, M. Trentin, J.M. Tarascon, Electrochem. Solid State Lett. 5 (2002) A286.
[4] K. Kanehori, K. Matsumoto, K. Miyauchi, T. Kudo, Solid State Ionics 9–10 (1983) 1445.
[5] S.D. Jones, J.R. Akridge, F.K. Shokoohi, Solid State Ionics 69 (1994) 357.
[6] J.B. Bates, N.J. Dudney, B. Neudecker, A. Ueda, C.D. Evans, Solid State Ionics 135 (2000) 33.
[7] Y. Iriyama, K. Nishimoto, C. Yada, T. Abe, Z. Ogumi, K. Kikuchi, J. Electrochem. Soc. 153 (2006) A821.
[8] http://www.excellatron.com/advantage.htm.
[9] J.B. Bates, N.J. Dudney, G.R. Gruzalski, R.A. Zuhr, A. Choudhury, C.F. Luck, J.D. Robertson, Solid State Ionics 53–56 (1992) 647.
[10] B.J. Neudecker, N.J. Dudney, J.B. Bates, J. Electrochem. Soc. 147 (2000) 517.
[11] S.-H. Lee, P. Liu, C.E. Tracy, Electrochem. Solid State Lett. 6 (2003) 275.
[12] S.S. Zhang, J. Power Sources 162 (2006) 1379.
[13] M. Hiratani, K. Miyauchi, T. Kudo, Solid State Ionics 28 (1988) 1406.
[14] W.-Y. Liu, Z.-W. Fu, Q.-Z. Qin, J. Electrochem. Soc. 155 (2008) A8.
[15] http://www.ohara-inc.co.jp/en/product/electronics/licgc.html.
[16] O. Loebich Jr., C.J. Raub, J. Less Common Met. 70 (1980) P47.
[17] C. van der Marel, G.J.B. Vinke, W. van der Lugt, Solid State Commun. 54 (1985) 917.
[18] T.B. Assalski (Ed.), Binary Alloy Phase Diagrams II, vol. 3, 1990, p. 2469.
[19] X. Yu, J.B. Bates, G.E. Jellison Jr., F.X. Hart, J. Electrochem. Soc. 144 (1997) 524.
[20] M. Paunovic, M. Schlesinger (Eds.), Fundamentals of Electrochemical Deposition, Wiley, New Jersey, 2006.
[21] W. Klemm, B. Volavsek, Z. Anorg. Allq. Chem. 296 (1958) 184.
[22] K. Terabe, T. Hasegawa, C. Liang, M. Aono, Sci. Technol. Adv. Mater. 8 (2007) 536.
[23] J. Suzuki, K. Sekine, T. Takamura, Electrochemistry 71 (2003) 1120.